JOURNAL OF KUFA−PHYSICS
www.uokufa.edu.iq/journals/index.php/jkp | ISSN: 2077−5830

Assessment of For Euphrates River In Al- Najaf Governorate Water Pollution Using Remote Sensing Data

*Hussain Muhyi Ali Zeena Yaseen Mahdy
University of Kufa/ Faculty of Education for Grils/ Physics Department
*Corresponding Author E-mail: husseinm.almusawi@uokufa.edu.iq

ARTICLE INF.:
Article history:
Received: 14 JUL, 2019
Accepted: 25 SEP, 2019
Available Online: 25 DEC, 2019

Keywords:
TSS
Shatt Al-Kufa
Remote sensing
Landsat 8 OLI.

ABSTRACT

Shatt Al- Kufa (Kufa River) is the major supply of surface waters in Najaf; Water pollution as a result of human activities Different .Water pollution results when contaminants are introduced into the natural environment. releasing inadequately treated wastewater into natural water bodies can lead to degradation of aquatic ecosystems In turn, this can lead to public health problems for people living downstream. They may use the same polluted river water for drinking or bathing or irrigation. Water pollution is the leading worldwide cause of death and disease due to water-borne diseases. The method used for modelling the TSS spatial distribution is the empirical modelling Conversion From image pixel values to reflectivity the reflectivity of each TSS concentration was extracted the reflection (r) on the X axis and the TSS concentration on the Y axis were extracted. The purpose of this study is to determine the estimated concentration of total suspended solid (TSS) in the Shatt Al- Kufa as the result of Landsat 8 OLI. As well by correlating the measured and estimated TSS and concentration the data used in this study was collected from Shatt Al- Kufa (10 stations) on 22 April 2019. In conjunction with the Landsat 8 OLI image data, obtained from the USGS site. The results revealed value of TSS in Shatt Al- Kufa can accurately using band 4 (red band).The determinant Coefficient between TSS field and reflectance value of image using band 4 is 0.785.Root Mean Square Error band 4 is 4.5225 ,mean relative error is 1.1649.

DOI: http://dx.doi.org/10.31257/2018/JKP/2019/110206

تقييم لنهر الفرات في محافظة النجف تلوث المياه باستخدام بيانات الاستشعار عن بعد

حسين محي علي زينة ياسين مهدي
جامعة الكوفة / كلية التربية للبنات / قسم الفيزياء

الـــخُـلاصـــة

الكلمات المفتاحية:

شط الكوفة (نهر الكوفة) هو المصدر الرئيسي للمياه السطحية في النجف. تتلوث المياه نتيجة للأنشطة البشرية المختلفة. ينتج تلوث المياه عند إدخال الملوثات في البيئة الطبيعية. يمكن أن يؤدي إطلاق مياه الصرف الصحي غير المعالجة إلى مسطحات مائية الطبيعية إلى تدهور النظم البيئية المائية ، وهذا بدوره يمكن أن يؤدي إلى مشاكل في الصحة العامة للأشخاص الذين يعيشون في اتجاه مجرى النهر. قد يستخدمون نفس مياه النهر الملوثة للشرب أو الاستحمام أو الري. وتلوث المياه هو السبب الرئيسي للوفاة والمرض في جميع أنحاء العالم بسبب الأمراض التي تنقلها المياه. الطريقة المستخدمة في التوزيع المكاني TSS وهي النموذج التجريبي لتحويل قيم بكسل الصورة إلى الانعكاسية ، تم استخراج الانعكاسية لكل تركيز TSS الانعكاس (r) على المحور X تركيز TSS على المحور Y. الغرض من هذه الدراسة هو تحديد التركيز المقدر للمواد الصلبة العالقة الكلية(TSS) في شط الكوفة لاندسات ٨ OLI. وكذلك عن طريق ربط TSS المقاسة والمقدرة. تم جمع البيانات المستخدمة في هذه الدراسة من شط الكوفة (١٠ محطات) في ٢٢ أبريل ٢٠١٩. بالتزامن مع بيانات صورة Landsat 8 OLI ، تم الحصول عليها من موقع هيئة المسح الجيولوجي الأمريكية. أظهرت النتائج أن قيمة TSS في شط الكوفة يمكن أن تستخدم بدقة النطاق ٤ (النطاق الأحمر). المعامل المحدد بين مجال TSS وقيمة الانعكاس للصورة باستخدام النطاق ٤ هو ٠.٧٨٥. Root Mean Square للحزمة ٤هو ٤.٥٢٢٥ ، mean relative error هو ١.١٦٤٩.

TSS
شط الكوفة
الاستشعار عن بعد
Landsat 8 OLI.

1. INTRODUCTION

Water pollution is a serious problem for human health and the environment,and all people require good drinking water quality to maintain their personal well-being. Drinking water should be aesthetically pleasant, clear, colourless and well aerated with no unpalatable taste and odour.

Microbiological, physical, chemical and radiological characteristics are also used to determine its suitability in terms of public health [1]. Shatt Al- Kufa (Kufa River) is the great supply of water needed for drink, irrigation, industry and applications other.. This river has shown decreasing quantity and quality of water because of population expansion and increased farming and urbanization; urban and farming wastes have been enlarged significantly and have made their way into the river. Issues with water quality have thus become more significant than quantity issues, making it necessary to conduct detailed studies to evaluate the suitability of this river for various purposes [2]. Currently, technology of remote sensing has been constantly evolving and can be used to sense water . Remote sensing data have been more used for oversight the ecological, physical, and biological state of the seawater [3]. The Landsat 8 satellite carries a two-sensor payload, the Operational Land Imager (OLI) and the Thermal Infrared Sensor (TIRS) (TIRS) that image the earth surface throughout the visible and thermal portions of the spectrum. [4]. and are summarized in Table 1. Landsat 8 has a 16 day repeat cycle; eachWRS-2 path/rowis overpassed every 16 days andmay be acquired a maximum of 22 or 23 times per year, as for Landsat 4, 5 and 7 [5]. And total suspended solid (TSS) as a focus measure of water quality [6 - 8].

Table 1: Landsat-8 (OLI) spectral band[9].

Band	Resolution (m)	Wavelength (μm)
B1-blue	30	0.43 - 0.45
B2-blue	30	0.45 - 0.51
B3-green	30	0.45 - 0.51
B4-red	30	0.64 - 0.67
B5-near infrared	30	0.85 - 0.88
B6-shortwave infrared	30	1.57-1.65
B7-shortwave infrared	30	2.11 - 2.29
B8-panchromatic	15	0.50 - 0.68
B9-Cirrus	30	1.36-1.38
B10-thermal Infrared(TIRS)	100	10.60-11.19
B11-thermal Infrared(TIRS2)	100	11.50-12.51

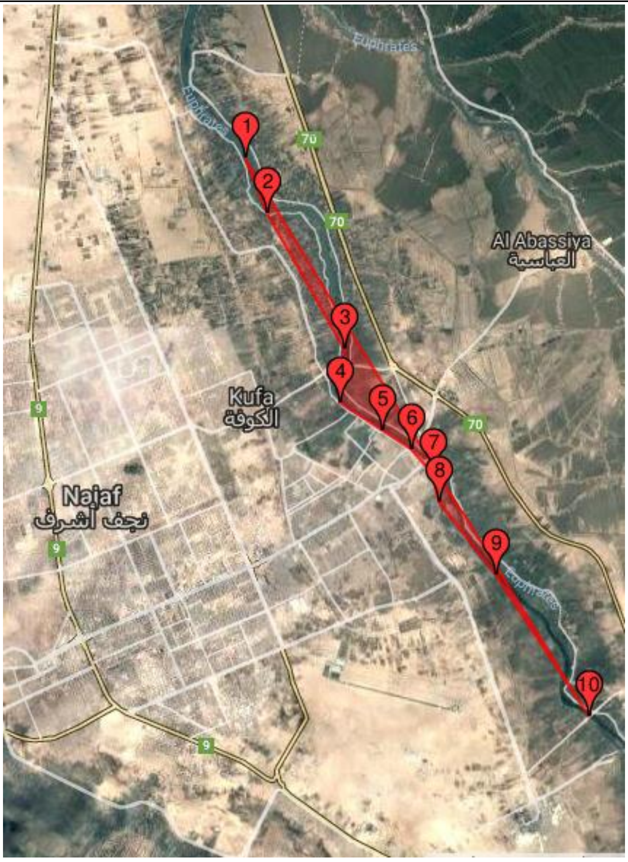

Figure 1: study area and Samples Location

2. MATERIALS AND METHODS

2.1 Study Area

The study area is located within Kufa district in Najaf province, 10 km .It located between the northern x/m (440485) y/m (3551386) to southern x/m (448061) y/m(3538978) in the Shatt Al-Kufa.as in Figure (1). The Euphrates River passes after the city of Kifl and divides the Euphrates River into two rivers: the Kufa Shat length and width of 73km and about 100m respectively, and Abbasid. The water level is unstable. The Shatt Al- Kufa surrounding areas are famous with farming [10]. This study includes 10 selected sites along the Kufa area (the most polluted area) started from the Zirka Cement Factory Bridge.

2.2 Sampling collection and Landsat 8 image

Samples were collected on 22 April 2019 , form 10 stations at a depth of about (30 cm) from the Zirka area and up to the bridge of the cement factory. Table (2), In conjunction with the Landsat 8 OLI image data, obtained from the USGS website [11].

Table 2: The table contains selected samples of the water of the Shatt Al- Kufa.

Location Stations	Code Stations	x/m	y /m	Temp.
Zirka area	S1	440485	3551386	26°
Al - Zarka Water Project	S2	440983	3550154	28°
Agricultural house towards Zarka area	S3	442685	3547150	28°
The Northern Incubator	S4	442563	3545953	25°
The Kufa Water Project	S5	443503	3545314	26°
Opposite Sikka Street	S6	444159	3544899	24°
Near the Palace of Hospitality	S7	444629	3544347	24°
The area of the animals	S8	444753	3543735	24°
Unit treatment of the Barakia station	S9	446017	3542118	26°
Cement Plant Bridge	S10	448061	3538978	24°

2.3 Regression Equation

Regression equation was used to obtain resultant regression function to model the TSS(Figure 2- 8) . The independent variable are the reflectance and the dependent variables are TSS field value. Regression Equation used was linear model equation . The main formula for the resultant regression function is as follow[12]:

$$\boldsymbol{y = ax + b} \dots\dots\dots\dots\dots\dots\dots\dots\dots\dots\dots\dots..(\mathbf{1})$$

Variables

y= The dependent variable (field TSS)

a= The constants

b= The slope of regression

x= The independent variables.

2.4 conversion of pixel values to reflectance

Radiometric correction function was used to equalize the solar conditions in each region/pixel in the image to get the reflectance value by changing the value of Digital Number (DN) into the reflectance value. This was completed by algorithm formula accord to USGS (2016) as follows[13]:

$$\boldsymbol{\rho_\lambda = M_\rho * Q_{cal} + A_\rho} \dots\dots\dots\dots\dots\dots\dots(2)$$

Where:

$\boldsymbol{\rho_\lambda}$= TOA (Top of Atmospheric) planetary reflectance, without correction for the solar angle.

$\boldsymbol{M_\rho}$= Band-specific multiplicative rescaling factor from the metadata.

$\boldsymbol{A_\rho}$= Band-specific additive rescaling factor from the metadata.

$\boldsymbol{Q_{cal}}$= Quantized and calibrated standard product pixel values (DN).

TOA reflectance was corrected based on the sun angle following formula as follow:

$$\boldsymbol{\rho_\lambda = \frac{\rho_\lambda}{\sin\theta_{SE}}} \dots\dots\dots\dots\dots\dots\dots(3)$$

where:

$\boldsymbol{\rho_\lambda}$= TOA planetary reflectance

θ_{SE} = Local sun elevation angle.

3. RESULT AND DISCUSSION

Table3. Relationship between TSS field concentration and reflectivity r band1-band7 for sample locations.

No. bands	Regression Equation	Correlation Coefficient(r)	Coefficient of Determination(R^2)
band1-Ultra-blue	***y = 951.53x - 102.34***	0.509	**0.259**
Band 2-Blue	***y = 560.9x - 49.558***	0.645	**0.416**
Band3-Green	*y = 485.38x - 33.933*	0.726	0.528
Band4-red	***y = 373.35x - 15.601***	0.886	**0.785**
Band5-NIR	***y = 315.97x - 13.881***	0.839	**0.704**
Band 6-SWIR 1	***y = 200.67x + 0.9417***	0.716	**0.513**
Band7-SWIR2	*y = 438.71x - 13.334*	0.835	0.697

In accordance with Table (3) where the correlation r) and the R2 coefficient between reflectivity and laboratory concentration TSS (mg / l) range between(0.509-0.886) (0.259-0.785), respectively. Band4-red is the highest correlation (r = 0.886) and R2 = 0.785). At the same time, band1-Ultra-blue is less correlated (r = 0.509).

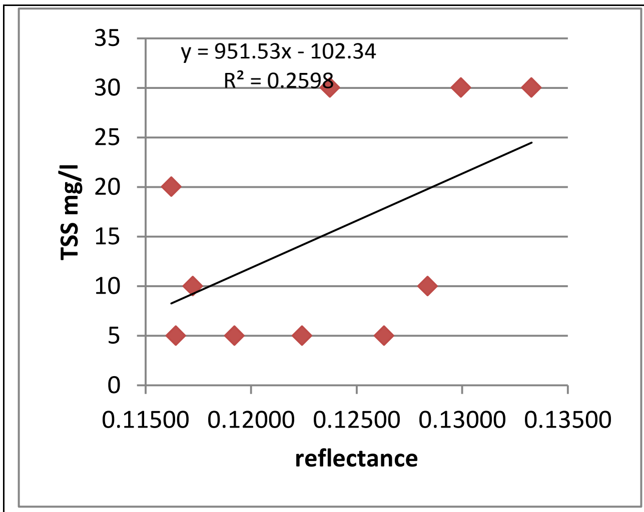

Figure 2. The relationship between spectral reflectivity and (TSS) of the band 1.

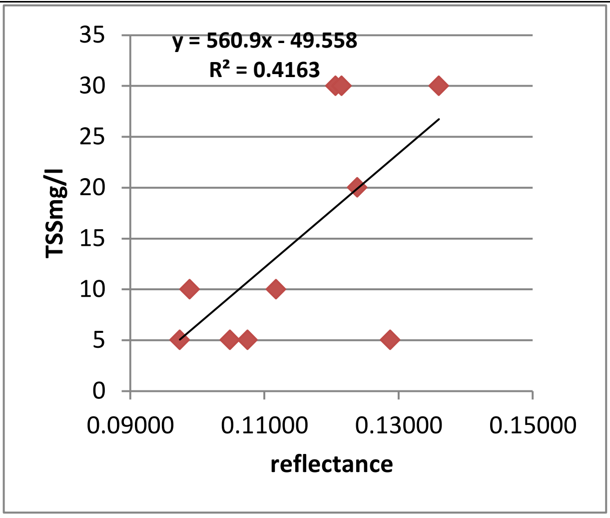

Figure 3. The relationship between spectral reflectivity and (TSS) of the band2.

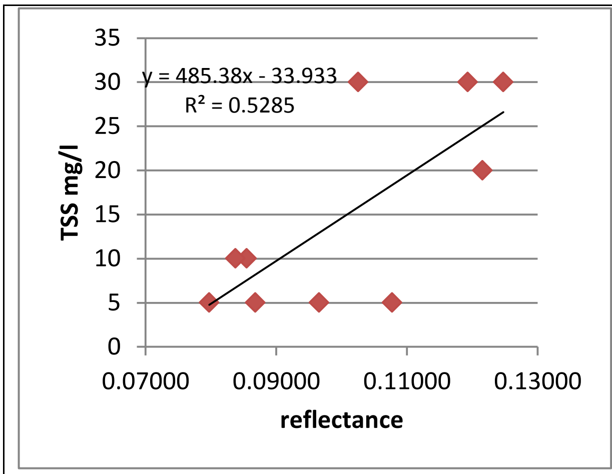

Figure 4. The relationship between spectral reflectivity and (TSS) of the band 3.

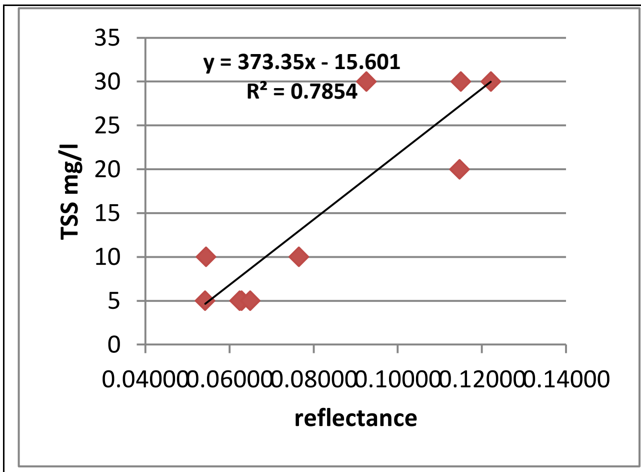

Figure5. The relationship between spectral reflectivity and (TSS) of the band 4.

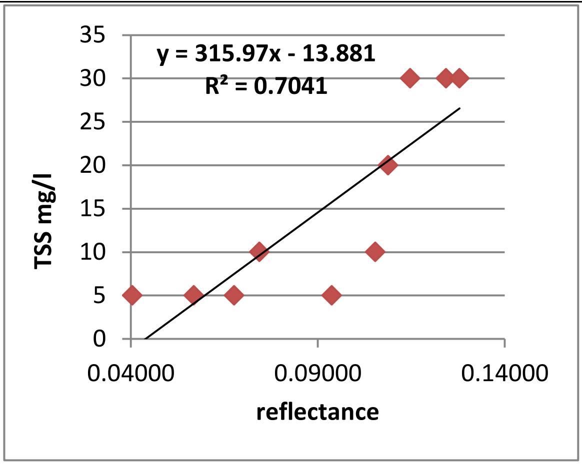

Figure6. The relationship between spectral reflectivity and (TSS) of the band 5.

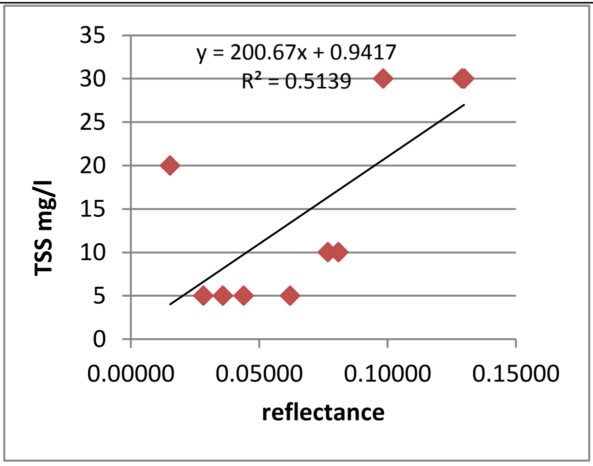

Figure7. The relationship between spectral reflectivity and (TSS) of the band 6.

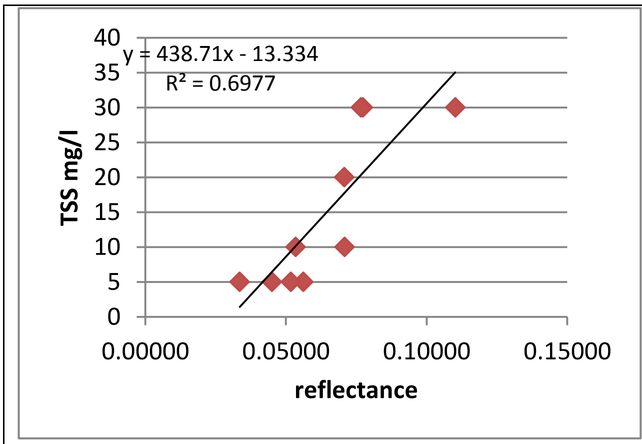

Figure8. The relationship between spectral reflectivity and (TSS) of the band7.

3.1 Distribution of TSS

Table4: The result of TSS estimation (mg/l) from each band

No. bands	MAX	MIN	MEAN	STD.
band1-Ultra-blue	77.6601	0.9746	14.4270	9.1515
Band 2-Blue	52.0412	0.0066	7.9235	6.8336
Band3-Green	56.9901	0.0001	6.5487	8.1446
Band4-red	61.9882	0.0027	7.5509	9.5034
Band5-NIR	111.1574	0.0030	18.7768	22.1574
Band 6-SWIR 1	59.6013	0.6802	12.7728	10.8378
Band7-SWIR2	100.6122	0.0086	10.9192	14.3266

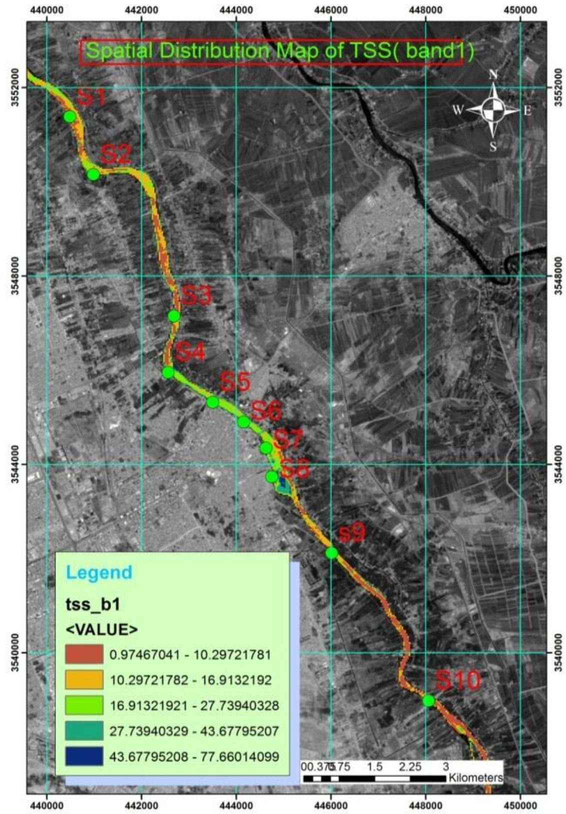

Figure9:The spatial distribution of TSS modeled from band 1.

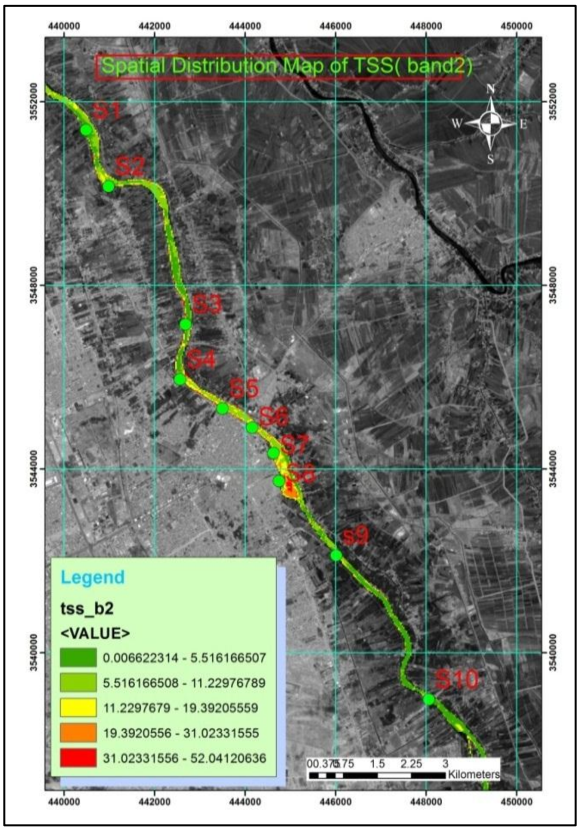

Figure10:The spatial distribution of TSS modeled from band 2.

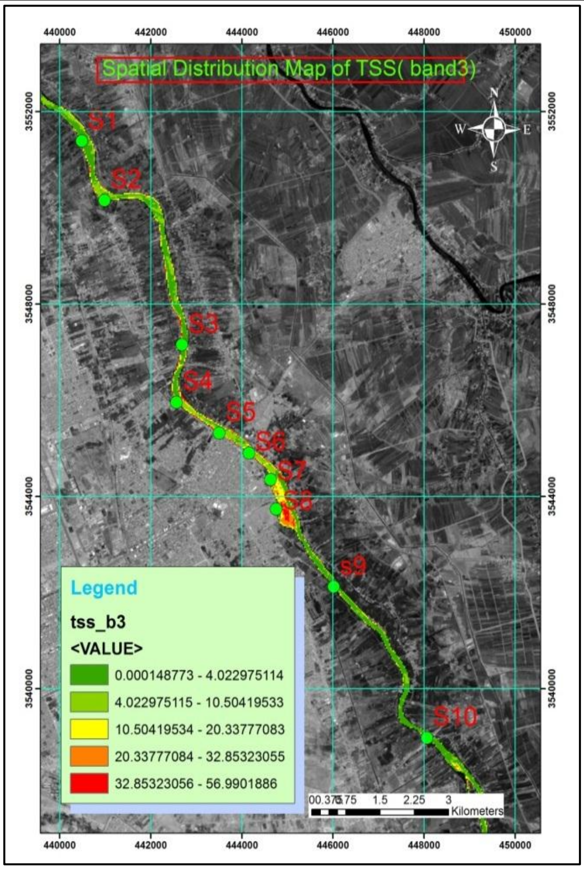

Figure11:The spatial distribution of TSS modeled from band 3.

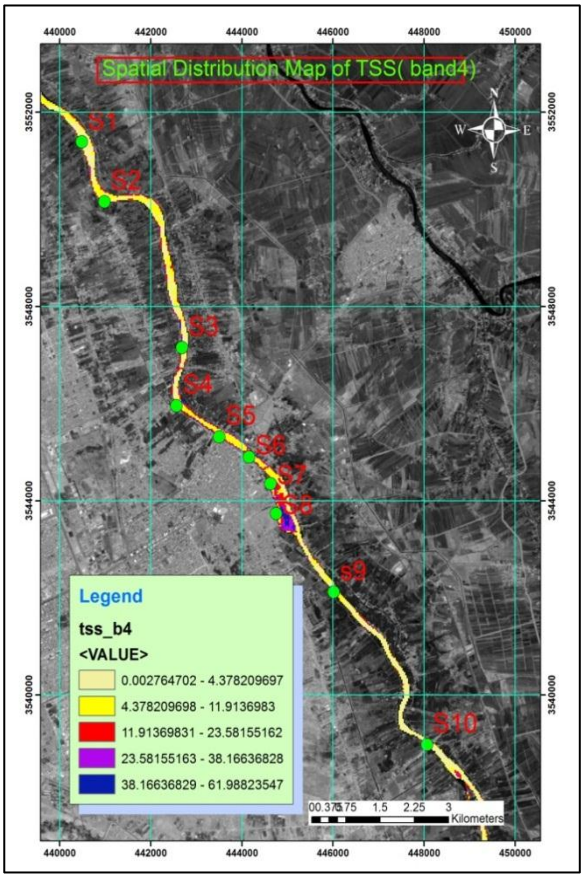

Figure12:The spatial distribution of TSS modeled from band4.

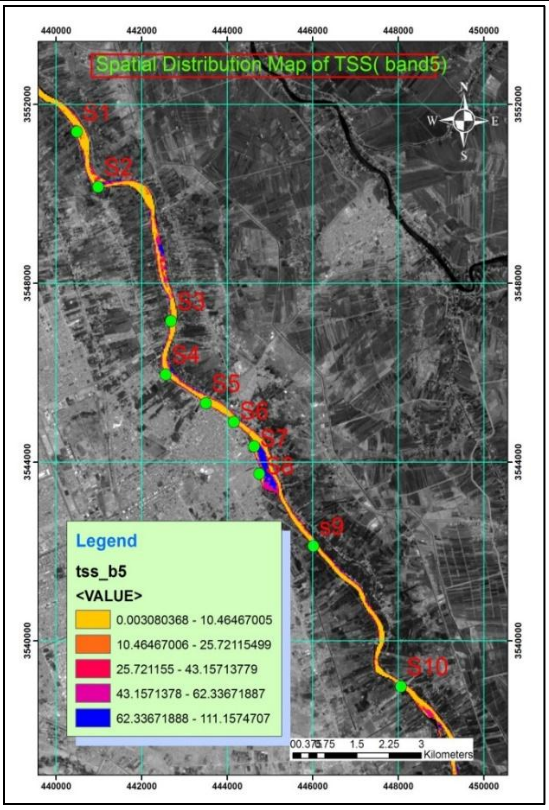

Figure13:The spatial distribution of TSS modeled from band5

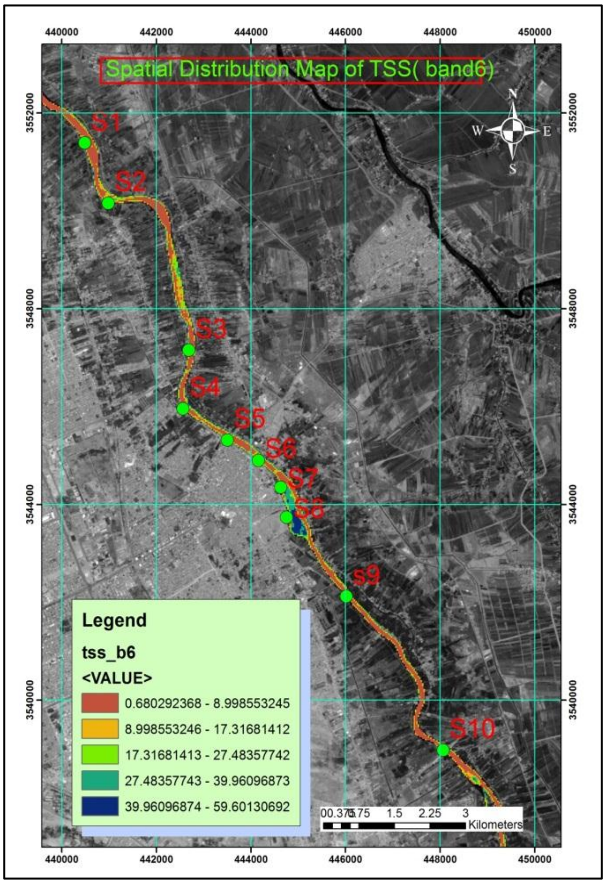

Figure15:The spatial distribution of TSS modeled from band6.

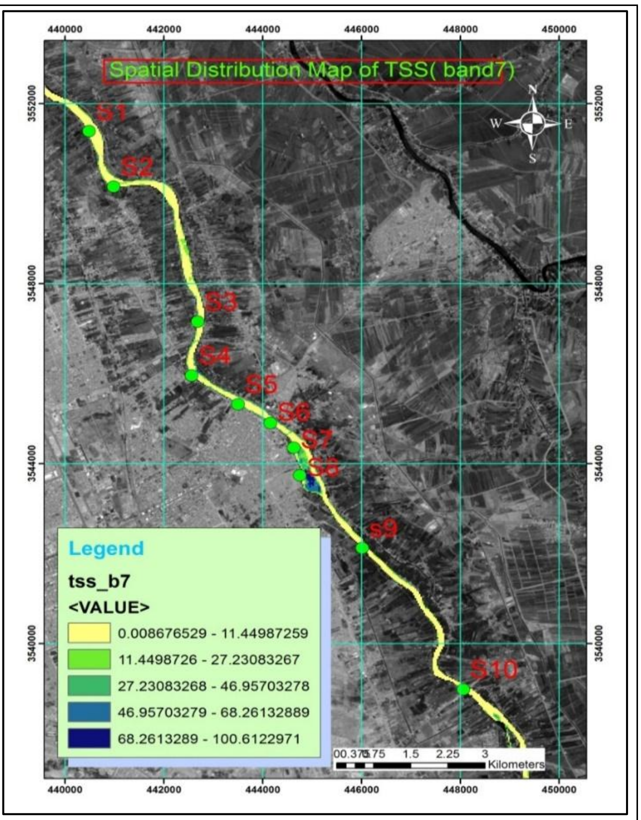

Figure16:The spatial distribution of TSS modeled from band7.

3.2 Accuracy Assessment

In order to validate the accuracy of the TSS spectral models, atmospheric correction and mapping of TSS concentrations, the most frequently used methods, the Root Mean Square Error (RMSE)and mean relative error (MRE), These notations were defined as follow[14]:

$$\boldsymbol{RMSE} = \sqrt{\frac{\sum_{i=1}^{n}(tss_{esti} - tss_{meas})^2}{N}} \quad \ldots\ldots\ldots\ldots\ldots (4)$$

$$\boldsymbol{MRE}(\%) = \frac{1}{N}\sum_{i=1}^{N}\left|\frac{tss_{esti} - tss_{meas}}{tss_{meas}}\right| * 100 \ldots (5)$$

where tss_{meas},i and tss_{esti},i are the measured and estimated values, respectively, and N is the number of samples.

Table 5: the accuracy results TSS(estimation (mg/l)

No. bands	*RMSE*	*MRE %*
band1-Ultra-blue	5.9427	1.6036
Band2-Blue	4.1748	1.4693
Band3-Green	4.6105	1.8067
Band4-red	2.697	1.1751
Band5-NIR	4.3493	1.6995
Band6-SWIR 1	3.4413	1.4951
Band7-SWIR2	3.8697	1.2402

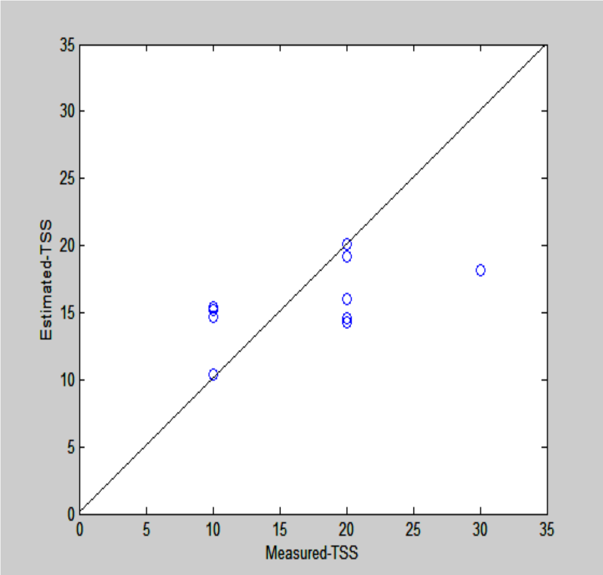

Figure 17: Estimated vs. Measured TSS Band 1.

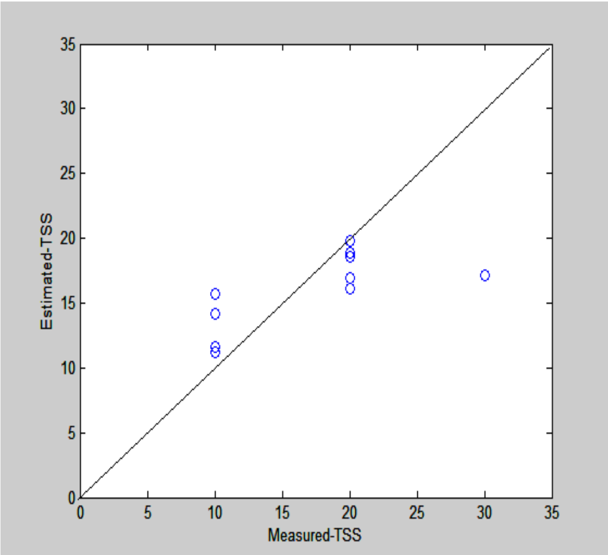

Figure 18 :Estimated vs. Measured TSS Band 2.

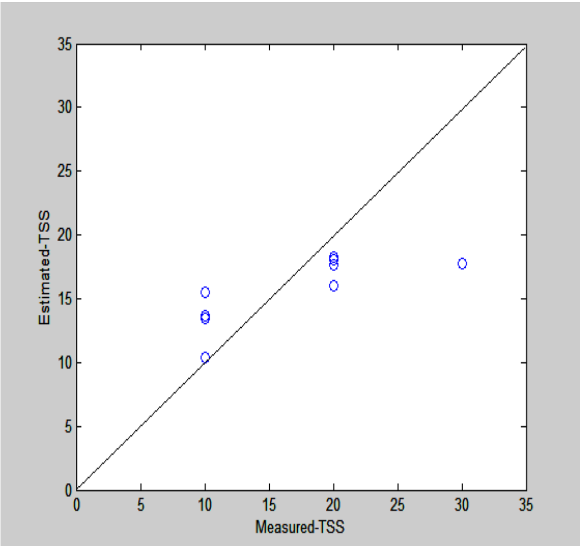

Figure 19: Estimated vs. Measured TSS Band 3.

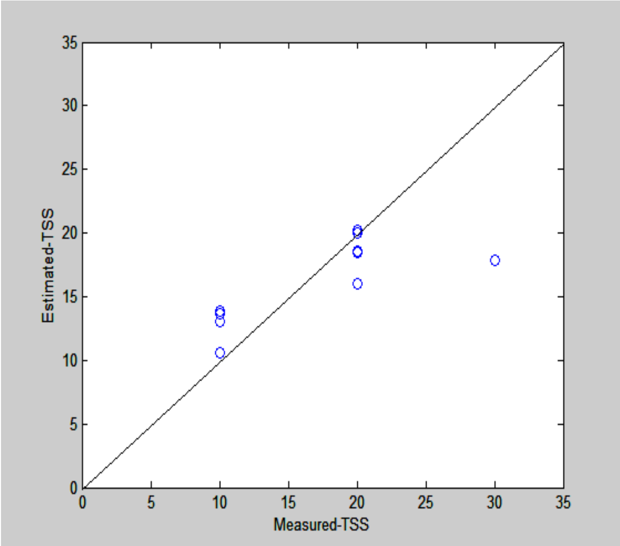

Figure20: Estimated vs. Measured TSS Band 4.

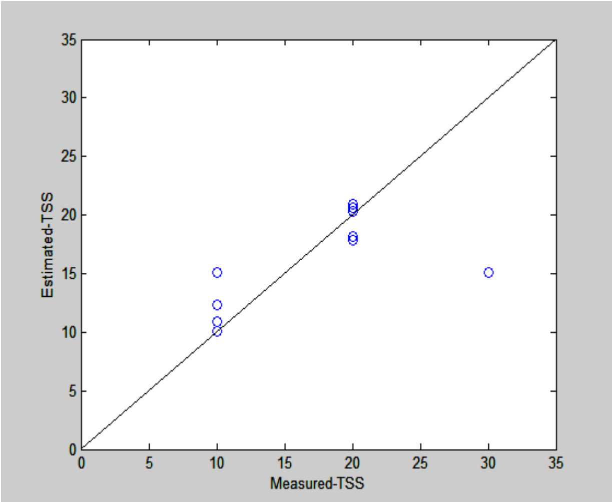

Figure21: Estimated vs. Measured TSS Band 5.

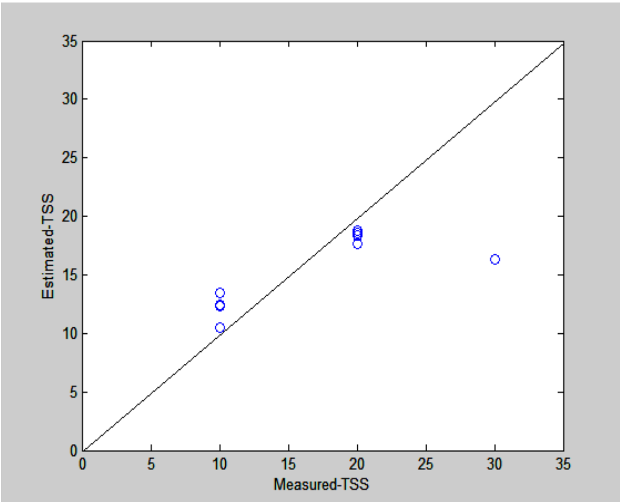

Figure22: Estimated vs. Measured TSS Band 6

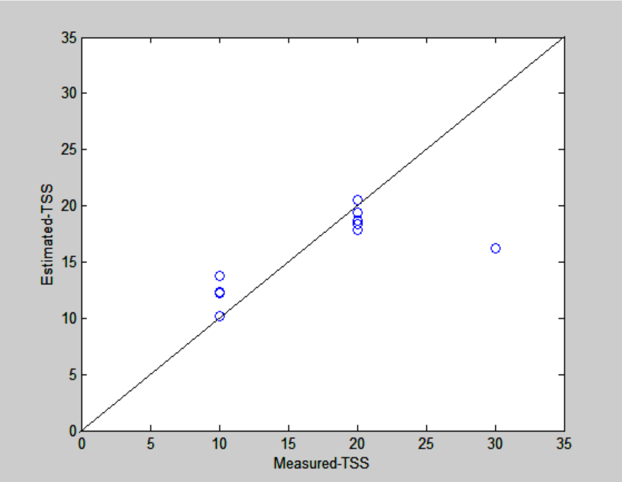

Figure23: Estimated vs. Measured TSS Band7.

3.3 Results of Accuracy Assessment

The accuracy assessment is plesented in (Table5). The accuracy assessment indicates that band 4 has the smallest deviation in the estimation of TSS image RMSE=2.697, and MRE %= 1.1751mg/l. Meanwhile, band with the highest deviation in estimating TSS is band 1 RMSE=5.9427, MRE %=1.6036 mg/l. This can be caused by the penetration ability and susceptibility to materials of TSS or object of water.

4. CONCLUSION

This research shows that Landsat 8 OLI band 4 has the best accuracy with (RMSE=2.697mg/l ,MRE =1.6995%). The distribution of TSS in Shatt Kufa on band 4 of Landsat 8 OLI has an estimated value of TSS as follow:(1, the lowest is 0.0027mg/l, 2 the highest is 61.9882 mg/l ,33) the average value is 7.5509 mg/l, 4 the standard deviation 9.5034). Analysis of the correlation between reflectivity (r) for the remote sensing data and TSS), the band (4) is the highest correlation with (r =0.886, R2 =0.785) and regression equation(y = 373.35x - 15.601). While band 1 was less correlation (r=0.509,R2 =0.259) and regression equation (y = 951.53x - 102.34).

5. REFERENCES

[1] Mohammed, Risala A. "Water Quality Index for Basrah Water Supply." Engineering and Technology Journal 31.8 Part (A) Engineering (2013): 1543-1555.

[2] Kizar, F. M. "A comparison between weighted arithmetic and Canadian methods for a drinking water quality index at selected locations in shatt al-kufa." IOP Conference Series: Materials Science and Engineering. Vol. 433. No. 1. IOP Publishing, (2018).

[3] Dekker, Arnold Graham. "Detection of optical water quality parameters for eutrophic waters by high resolution remote sensing." (1993).

[4] Pahlevan, Nima, and John R. Schott. "Investigating the potential of the operational land imager (OLI) for monitoring case II waters using a look-up-table approach." Pecora 18: Forty Years of Earth Observation—Understanding a Changing World (2011).

[5] ovalskyy, V., and David P. Roy. "The global availability of Landsat 5 TM and Landsat 7 ETM+ land surface observations and implications for global 30 m Landsat data product generation." Remote Sensing of Environment 130 (2013): 280-293.

[6] Binding, C. E., D. G. Bowers, and E. G. Mitchelson-Jacob. "Estimating suspended sediment concentrations from ocean colour measurements in moderately turbid waters; the impact of variable particle scattering properties." Remote sensing of Environment 94.3 (2005): 373-383.

[7] Chen, Zhiqiang, Chuanmin Hu, and Frank Muller-Karger. "Monitoring turbidity in Tampa Bay using MODIS/Aqua 250-m imagery." Remote sensing of Environment 109.2 (2007): 207-220.

[8] Martinez, Jean-Michel, "Increase in suspended sediment discharge of the Amazon River assessed by monitoring network and satellite data." Catena 79.3 (2009): 257-264.

[9] Roy, David P. "Landsat-8: Science and product vision for terrestrial global change research." Remote sensing of Environment 145 (2014): 154-172.

[10] Abdulmuttaleb, Hussein. "Evaluation of Surface Water Quality in Al Kufa River Station Al-Qadisiya J." Eng. Sci 5 (2012): 451-65.

[11] The website: http://remotesensing.usgs.gov.

[12] Yanti, Apriwida, Bowo Susilo, and Pramaditya Wicaksono. "The aplication of Landsat 8 OLI for total suspended solid (TSS) mapping in Gajahmungkur reservoir Wonogiri regency 2016." IOP C Ser Earth Env 47 (2016): 012028.

[13] Wisha, Ulung Jantama, Ruzana Dhiauddin, and Gunardi Kusumah. "Remote Esti mation of total Suspended Solid (TSS) Transport Affected by Tidal Bore “Bono” of Kampar Big River Estuary Using Landsat 8 OLI Imagery." Marine Research in Indonesia 42.1 (2017): 37-45.

[14] Wang, Chongyang, "A Landsat-based model for retrieving total suspended solids concentration of estuaries and coasts in China." Geoscientific Model Development 10.12 (2017).